

# OPTICS AND SPECTROSCOPY

Founded by Ioffe Institute

Published since January 1956, 12 issues annally

Editor-in-Chief: Nikolay N. Rosanov

Editorial Board:

Tigran A. Vartanyan (Deputy Editor-in-Chief), Evgenii B. Aleksandrov, Pavel A. Apanasevich, Igor A. Bufetov, Mikhail I. Dyakonov, Sergey Ya. Kilin, Marina N. Popova, Vladimir M. Shabaev, Ivan V. Sokolov, Valery V. Tuchin, Anton K. Vershovskii, Valerii S. Zapasskii

*ISSN: 0030-400X (print), 1562-6911 (online)*

OPTICS AND SPECTROSCOPY is the English translation of  
ОПТИКА И СПЕКТРОСКОПИЯ (ОПТИКА I SPECTROSKOPIYA)

Published by Ioffe Institute

# Radiation of plasma diffuse jets in the wavelength range of 120–1000 nm at air pressures of 0.2–1.5 Torr

© V.F. Tarasenko, A.N. Panchenko, E.Kh. Baksht, N.P. Vinogradov

Institute of High Current Electronics, Siberian Branch, Russian Academy of Sciences, Tomsk, Russia

e-mail: VFT@loi.hcei.tsc.ru

Received November 01, 2024

Revised December 24, 2024

Accepted January 22, 2025

At present, studies of various atmospheric discharges in the stratosphere and mesosphere are ongoing. Considerable attention is paid to the study of the spectral characteristics of the radiation of red sprite plasma, including columnar ones. However, field studies require large material costs. Therefore, in parallel, work is being carried out on experimental modeling of the properties of high-altitude discharges in laboratory conditions at low atmospheric air pressures. The article presents the results of studies of the spectral properties of plasma diffuse jets (PDJs), which are analogs of columnar sprites. PDJs were formed using a pulse-periodic barrier discharge in quartz tubes at pressures of 0.2–2 Torr in air and nitrogen. In the spectral range from 120 to 1000 nm, data were obtained on the relative spectral density of radiation energy on three bands of the nitrogen molecule and one band of the molecular nitrogen ion both from the end of the quartz tube and from its side surface. It was found that in the emission spectra of the PDS from the end of the tube and its side surface near the electrodes, the intensity ratio of the bands of the second positive (2+) and first negative (1-) nitrogen systems changes in favor of the 1-system. Radiation was recorded in the vacuum-ultraviolet region of the spectrum on the  $a^1\Pi_g - X^1\Sigma_g^+$  band of nitrogen molecules and on the lines of atomic nitrogen, the intensity of which increased with decreasing air pressure. It was confirmed that in the PDS, the spectral density of the radiation energy  $W$  of the 2+ nitrogen system bands exceeds the  $W$  of the 1+ nitrogen system bands.

**Keywords:** plasma diffuse jets, air, nitrogen, low pressure, emission spectra, VUV lines and bands, intensity ratio.

DOI: 10.61011/EOS.2025.01.60560.7284-24

## Introduction

Currently, studies of electrical discharges in the stratosphere and mesosphere which are called „transient luminous events“ (TLE) are continued [1,2]. In particular, the emission spectra of various types of discharges are studied in detail, for example, red sprites (specific type of lightning occurring in the upper layers of Earth atmosphere during large thunderstorm at high altitudes), blue jets, elves, halo and other more rare kinds of discharges [3,4]. Research is carried out both in the ground-based laboratories on Earth [5] and in the airborne „flying“ laboratories [6]. In addition, spectral instruments are installed on the satellites [7] and the International Space Station [8]. The greatest attention is paid to the study of column red sprites, photographs of which, as well as their emission spectra, can be found in many papers [9–11]. Red sprites are observed at altitudes 40 to 100 km above the sea level. The column sprites occur at an altitude of 85 km and have a more simple structure [1–4]. Their length exceeds 10 km and they may change their shape and color when propagating towards the Earth surface [11]. To date, it has been established that the formation of column sprites occurs during lightning discharges due to streamers, which are usually initiated at the bottom of the halo. Sprites are formed mainly when positive lightning occurs between the cloud and the Earth. A streamer (a movable gas ionization area generated

by high electric current at the front of a dense plasma), which induces the major sprite channel, by propagating downwards may generate a glow, and beads below this area. Further, it can be divided into several streamers with a smaller channel diameter. It has been found that the glow region, which is located in the upper part of the sprite, has the highest intensity in the red sprites radiation [3].

It has now been unambiguously established [1–3,11] that the red color of the sprites is explained by radiation of bands of the nitrogen molecules first positive system (1+). The blue hue in the sprites bottom region emission at an altitude of less than 50 km above sea level is provided by the bands of the first negative system (1-) of molecular nitrogen ion and the second positive system (2+) of nitrogen molecules [3,6,12]. Changes in the emission spectra of red sprites are usually observed in areas when their shape changes. So, in paper [12] it was shown when the altitudes go down from 60 to 50 km the intensities ratio of the band with a wavelength of 427.8 nm (1-) to the band with a wavelength of 337.1 nm (2+) increases. However, there is currently no or very little experimental data on the ratio of emission intensities in the vacuum ultraviolet (VUV), ultraviolet (UV), visible and near-infrared (IR) spectral regions obtained with high spectral resolution for column red sprites and other TLE. One of the reasons is the significant absorption of atmospheric gases [13], as well as

clouds and aerosols. This makes it much more difficult to register the emission spectra of natural discharges.

From theoretical modeling, it follows [11,14] that when air is excited in a quasi-static electric field, at least five bands of molecular nitrogen in the region of 120–1000 nm should be present in red sprites radiation. The study [14] describes the synthetic spectra for the systems of 1+, 2+, 1-, Lyman-Birge-Hopfield (LBH) and Mendel bands at  $N_2^+$  transitions, and also radiance analysis at four given values of electrical field strength ( $E/N = 20, 100, 200$  and  $400$  Td, where  $E$  — electrical field strength,  $N$  — particles concentration). It is assumed that the data obtained will be useful in measuring the energy put in red sprites.

Paper [15] provides the calculated data on the luminescence intensity of LPH bands, as well as 2+ band of the nitrogen system under air excitation by an electron beam with an energy from 10 keV to 10 MeV. It has been found that as the electron energy increases, the contribution of quenching the  $a^1\Pi_g$  state goes high in molecular collisions. This leads to a lower ratio of the integral luminescence intensities of LBH bands and the second positive system with the electron energy rise.

In parallel with the in-situ measurements of the radiation spectra in red sprites and theoretical computations, their analogues were experimentally simulated in laboratories [16–18]. However, in these studies, the generated plasma came into contact with metal electrodes, and the LBH band was not detected.

The properties of column red sprites were reproduced most closely to the real ones in studies [19–22], where red diffuse plasma jets (PDJ) with a length of more than one meter were created using a repetitively-pulsed barrier discharge. The PDJ were shown to be initiated from plasma that doesn't have any contact with metal electrodes due to both, positive and negative streamers [22]. It was also found that the red color of the discharge, which is visually observed and obtained by photographing with standard digital devices, is detected at the spectral emission energy density of the most intense bands 1+ of nitrogen system by 2 orders less than the energy density of bands 2+ of the nitrogen system. [19–21]. Experiments described in [19–22] were specially carried out at a high pulse repetition rate. This apparently made it possible, due to axial compression of the plasma by a surface charge, to obtain a cylindrical-shaped, meter-long PDJ at low voltages. Charges accumulated on the inner wall of the quartz tube due to operation in a repetitively-pulsed mode and stabilized the transverse dimensions of PDJ. Moreover, gas heating is influencing the PDJ diameter in the repetitively-pulsed mode. However, in these studies, spectral studies in VUV wavelength range were not carried out, and the emission intensity of LBH band of the nitrogen molecule was not compared with other bands.

The purpose of this study is to examine the emission spectra of PDJ (which are miniature analogues of red sprites) in the range of 120–1000 nm, and to obtain data on the ratio of molecular nitrogen bands intensities in various

wavelength ranges, and also to detect VUV emission of LBH bands.

## Experimental setup and measurement techniques

To get PDJ emission spectra in VUV spectrum an experimental setup was organized shown in Fig. 1, *a*. The discharge was formed in the tube 2 when a high-voltage generator with an amplitude of no-load voltage pulses  $U \sim 10$  kV was connected to the annular external electrodes 3, 4. In the repetitively-pulsed mode ( $f = 1$  kHz and higher) with the voltage pulse duration at half maximum  $\sim 1.5 \mu s$   $U$  was reduced to  $\sim 7$  kV. The duration  $U$  of the pulse front and droop were the same and during formation of PDJ were  $\sim 350$  ns. Either electrode 4, or electrode 3 could be used as high-voltage electrodes made of  $100 \mu m$  thick aluminum foil. The width of these electrodes was 1 cm. The generator generated high voltage pulses of both negative and positive polarity. The emission spectra were usually recorded at a pulse repetition rate of 2 kHz. The discharge tube was made of GE-214 quartz glass featuring a high transmittance in UV, visible and near-infrared regions of the spectrum. The length of the tube, its inner diameter and walls thickness were 64 cm, 5 cm and 2.5 mm, respectively. The axis of the tube was located at a distance of 18 cm from the flat metal surface of the experimental stand. To obtain the emission spectra in VUV spectra, the right end (if looking straight) of the tube 2 was connected to a stainless steel transition chamber 5 with a window 6 of  $MgF_2$ . The transition chamber was grounded and connected to a monochromator, the entrance slit of which received radiation from the axial part of the discharge. The left end of the quartz tube was closed with a flange 1 made of a dielectric with a fitting 9, through which the air was pumped out from the tube and pumped in from the laboratory room. High-purity nitrogen was used instead of air in some experiments. Upon receiving data for each set of conditions, the tube was pumped out by a pre-vacuum pump to  $p = 10^{-2}$  Torr, and then filled with air or nitrogen to the desired pressure. Relative air humidity in the room before it was pumped into the tube was  $\sim 23\%$  at a temperature of  $22^\circ C$ .

Discharge plasma emission spectra in the region of 120–550 nm were recorded using a vacuum monochromator VM-502 (Acton Research Corp.). The temporal characteristics of the radiation in individual spectral ranges were determined using PMT monochromator (EMI 9781 B) with a temporal resolution of  $\sim 3$  ns for the signal front edge and  $\sim 30$  ns for its trailing edge. To register the radiation spectra through the lateral surface of the quartz tube, HR2000+ES and HR4000 spectrometers (both manufactured by OceanOptics Inc.) equipped with a light guide were used. The sensitivity of the spectrometers and the transmission of the optical fiber in the range of  $\Delta\lambda = 250$ –1000 nm were known. Spectral resolution of

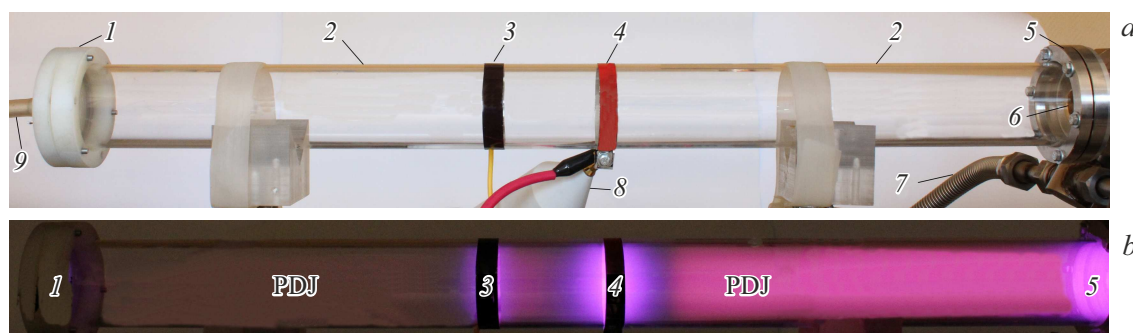


**Figure 1.** Photos of a setup for detection of PDJ (*a*) and discharge emission at negative generator polarity and air pressure  $p = 0.3$  Torr (*b*). 1 — left end-face caprolon flange of the tube, 2 — quartz tube, 3 — grounded electrode, 4 — high-voltage electrode, 5 — end of transition chamber for connection to the monochromator, 6 — window from  $\text{MgF}_2$ , 7 — hose for air pumping out from the transition chamber, 8 — voltage divider, 9 — nozzle to pump air in and out of the tube 2. Pulse repetition rate was  $f = 2$  kHz.

the optical system fitted with VM-502 monochromator was no worse than  $\sim 0.4$  nm at the width of the entrance slit of  $100\ \mu\text{m}$ , and that of the optical system with HR2000+ES and HR4000 spectrometers no worse than  $\sim 0.9$  and  $\sim 0.2$  nm respectively. Shooting of the integral glow of the discharge plasma was carried out with a Canon 2000D digital camera (CANON). The recording of the radiation spectra, as well as shooting the glow of the discharge plasma, was carried out in the dark.

The voltage across the discharge gap was measured using a TT-HVP 2739 high-voltage probe with a bandwidth of 220 MHz (8), and the discharge current — using a shunt based on TVO brand resistors having a resistance of  $0.1\ \Omega$ . The signals from the voltage divider and current shunt were detected by a digital oscilloscope Tektronix MDO 3104 (1 GHz, 5 GS/s).

## Measurement results

A photograph of the integral glow of the discharge in air at a pressure of 0.3 Torr is shown in Fig. 1, *b*. Plasma diffuse jets, as in papers [19,21,22], propagate in both directions from the plasma of the capacitive discharge between the electrodes 3, 4. Their occurrence is practically independent of the polarity and position of the high-voltage electrode (left or right). However, their brightness and shape are significantly affected by the gas pressure, the distance to the ends of the quartz tube and the material of the flanges, as well as the presence of grounding at the metal flange and the inductance of this grounding. In experiments with a vacuum monochromator, the PDJ had a higher brightness (in Fig. 1, *b* it is indicated as right PDJ), which propagated towards the transition chamber 5. This is due to an increase in the discharge current in this circuit after passing through the front of the streamer, which formed the PDJ, due to the grounding of the transition chamber 5. The streamers propagation in PDJ is described in detail in papers [21,22]. It should be noted that PDJ glow is relatively uniform in length, as is the glow of most column sprites. The air

pressure and length of the quartz tube for the conditions in Fig. 1, *b* were chosen relatively small and the PDJ reached both ends, while their diameter in these conditions was equal to the inner diameter of the quartz tube. However, as already noted, the intensity of discharge plasma radiation between the electrode 4 and the transition chamber 5 was significantly higher due to the grounding of the chamber.

Intensity of the discharge plasma glow for the high-voltage electrode 4 was higher (Fig. 1, *b*) than that of the grounded electrode 3. When changing the connection point of the generator's high-voltage output from the electrode 4 to the electrode 3, the emission intensity at the electrode 3 increased, and that at the electrode 4 decreased. Also, it should be stressed that between the bright glow at the electrode 4 and the right PDJ, as well as on its left side between the electrodes 3 and 4, the discharge glow areas have a lower radiation intensity. In addition, the color of the discharge between the dark area and the electrode has a blue color. It was found that in these areas, the color of the discharge is determined by the magnitude of the induced electrical field. The change in the reduced electric field was determined from the emission spectra of these regions, where the ratio of the intensity of 2+ and 1- bands of nitrogen systems from different parts of the quartz tube was measured. As known, see papers [20,21], in the region of an enhanced electric field, the spectral emission energy density  $W$  of 1- bands of the molecular nitrogen ion system (the most intense bands 391.4 and 427.8 nm) goes up. At the same time, the ratio of the intensities of nitrogen ion bands with a wavelength of 391.4 nm to the band 2+ of the nitrogen molecule system with a wavelength of 394.3 nm also increases, which indicates a higher electron temperature in the regions near the sharp edges of the ring electrodes.

Figure 2 shows the oscillograms of voltage pulses between the ring electrodes, as well as the discharge current when connecting the high-voltage output of the generator with a negative polarity to the electrode 3. Distances between the electrode 3 and flange 1, as well as between the electrode 4 and transition chamber 5 were almost the same (Fig. 1, *a*) and were equal  $\sim 28$  cm. Changing the

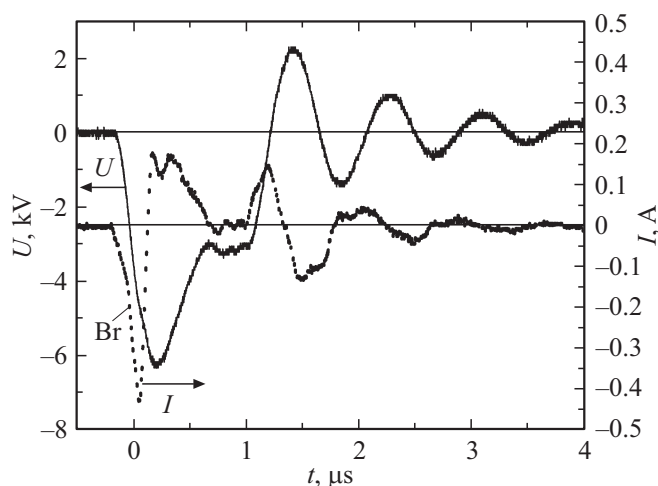


**Figure 2.** Oscillograms of voltage  $U$  pulses between the ring electrodes and discharge current  $I$  in the generator grounding circuit at the air pressure of 0.6 Torr and  $f = 2$  kHz.

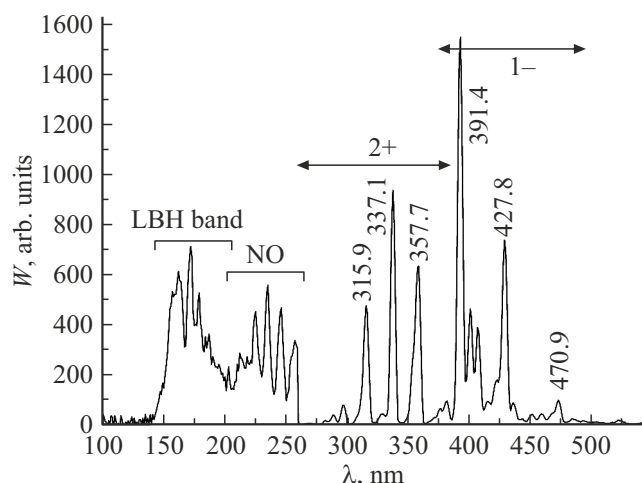


**Figure 3.** Spectral density of emission energy  $W$  when there's a discharge in the air from the axial part of the tube.  $p = 0.35$  Torr,  $f = 2$  kHz. LBH — Lyman-Birge-Hopfield bands. The intensity of emission in 100–260 nm was increased 25 times. Entrance slit of monochromator  $100\mu\text{m}$ .

position of the high-voltage electrode did not significantly affect the shape of these pulses. The breakdown between the electrodes 3,4 occurred approximately in 150 ns after supply of the voltage pulse. Capacitance current was detected before the voltage breakdown. An increase in the discharge current during the breakdown is indicated in Fig. 2 as Br dot. At this point, the rate of discharge current growth increased, and the voltage growth slowed down. Since the discharge between the electrodes 3,4 was limited by the walls of the quartz tube as a dielectric barrier, the voltage across the gap continued to rise after the breakdown and with the growth of plasma conductivity in the tube area 2 between the electrodes. Note that when operating in the repetitively-pulsed mode, the maximum voltage value

between the electrodes decreased compared to single pulses, and the pulse duration increased at half maximum. The measurements also showed that a change in the polarity of the high-voltage electrode at constant frequency of voltage pulses in units of kilohertz or more, as well as air pressure in the range (0.2–2), Torr does not significantly affect the shape of the voltage and current pulses.

The main purpose of this paper, as already mentioned, was to study the emission spectra of a discharge and determine the relative intensity of various bands during PDJ formation, and also to detect LBH bands in VUV region of the spectrum. Figure 3 shows the emission spectrum of a discharge in air from the near-axial part of the tube in the range from 120 to 550 nm, obtained using a VM-502 monochromator. The short-wave boundary of the monochromator was checked by studying the second argon continuum, the detected band of which had a maximum at a wavelength of 126 nm [23]. The emission spectrum in Fig.3 the bands 1- and 2+ of the nitrogen system are prevailing, although most of the tube is filled with PDJ glow, which has a red color. The intensity of PDJ glow on the right side was significantly higher than on the left, which is due to the short circuit of the discharge current to the grounded transition chamber. As known, in sprites [4,11], as well as in PDJ [19–21] the red color is defined by emission 1+ of the nitrogen system which was not included in the sensitivity region of this monochromator. Further in the article, the spectra will be presented, which will show the emission bands 2+, 1- and 1+ of nitrogen systems obtained with HR2000+ES spectrometer, as well as the photograph of a discharge with two PDJs. Formation of two PDSs oriented in different directions from the plasma created by a capacitive discharge between two external electrodes is explained by the fact that there's an approximately equal potential in the area between the electrodes, and the electrodes from both ends of the quartz tube are also removed. As it was shown in paper [20], when installing electrodes at the end of the quartz tube, the PDJ spread only in one direction.

The LBH bands and atomic nitrogen lines in VUV region of the spectrum, as well as NO bands in the area of 200–300 nm, had a relatively low spectral energy density  $W$ . Fig. 3 illustrates their intensity increased in 25 times. The main reason for low intensity of LBH bands emission is the absorption of VUV emission by oxygen molecules in the region shorter than 200 nm [24]. Therefore, it is somewhat difficult to detect these bands in the emission spectra of red sprites. However, when modeling the discharge of sprites, calculations show their presence at low air and nitrogen pressure [14]. In addition, their presence is confirmed by experiments cited in [11].

Fig. 4 illustrates the air and nitrogen emission spectra in the region of 120–200 nm detected using VM-502 monochromator at the entrance slit width of  $25\mu\text{m}$ . The emission spectrum in nitrogen was taken to show the effect of oxygen on the intensity of PDJ emission in VUV region of the spectrum. The LBH bands of nitrogen molecules and

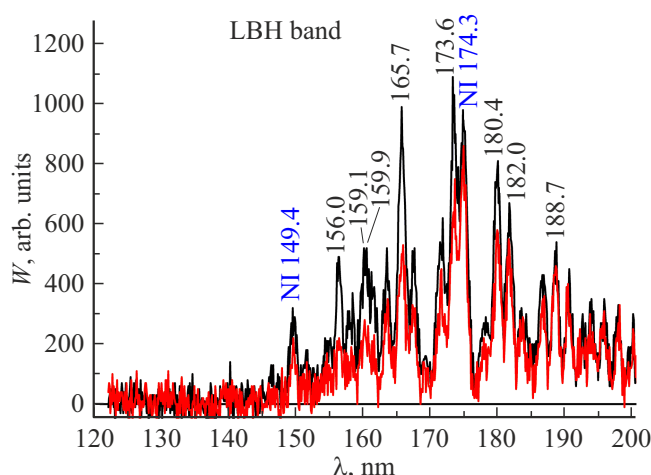


**Figure 4.** Spectral density  $W$  of charge emission in the air (red lines) and in nitrogen (black lines) from the axial part of the tube.  $p = 0.6$  Torr,  $f = 2$  kHz. Width of the monochromator entrance slit  $25\ \mu\text{m}$ . Black wavelength designations are used for the Lyman-Birge-Hopfield (LBH) molecular bands, blue for the atomic nitrogen lines.

atomic nitrogen lines were recorded both in air and nitrogen. However, they were less intense in the air compared to nitrogen. The relatively small difference in the intensity of bands and lines obtained in these experiments is due to the admixture of molecular oxygen to nitrogen, which was absorbed on the walls of the quartz tube and the pumping hose, and then released after ignition of the discharge. In the long-wavelength part of VUV spectrum (190–200 nm), where the absorption of molecular oxygen is still relatively low, the intensities at individual transitions of LBH band in air and nitrogen practically coincided in these conditions. The detected emission of atomic nitrogen lines is associated with the effective dissociation of  $\text{N}_2$  molecules when excited by an electric discharge under conditions of a high reduced electric field (over 100 Td). It is known that in pulsed discharges of atmospheric pressure with high overvoltage, intense radiation of atomic lines and atomic nitrogen ions is detected [25].

Figure 5 shows the dependences of  $W$  on air pressure for an atomic nitrogen line with a wavelength of 174.3 nm, which is produced in a discharge tube during the dissociation of nitrogen molecules. For all three curves, a decrease in air pressure led to an increase in the spectral energy densities of nitrogen emission lines from PDJ. Such dependencies were also true for LBH bands, where the change in  $W$  occurred together with the change in  $W$  for atomic nitrogen lines with the wavelengths 174.3 and 149.4 nm.

Spectral densities of emission energies in PDJ for 2+ and 1+ nitrogen systems, as well as for 1- and 2+ were compared with the use of a 220 cm long quartz tube with the same wall thickness, diameter and grade of the quartz glass GE-214. A photograph of the discharge in this series

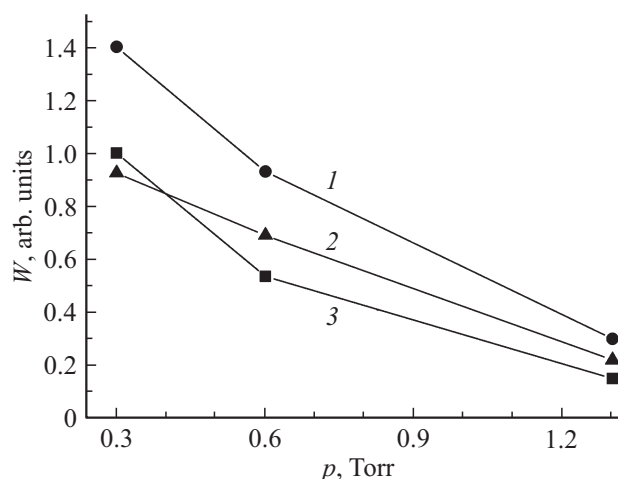


**Figure 5.** Curves of emission energy spectral density  $W$  for atomic nitrogen lines with the wavelength of 174.3 nm versus pressure, obtained under positive (1, 2) and negative (3) polarities of the high-voltage electrode when the high-voltage generator is connected to electrode 4 (1, 3) and to electrode 3 (2). Width of the monochromator entrance slit is  $25\ \mu\text{m}$ .  $f = 2$  kHz.

of experiments is shown in Fig. 6. The ring electrodes 3, 4 similar as in Fig. 1 were placed at a distance of 6 cm from each other. They were fabricated from a  $100\ \mu\text{m}$  thick foil and were 1 cm wide, but were placed at some distance from the ends of the quartz tube. The electrode 3 was removed from the left (relative to the reader) end flange by 63 cm and from the right, which is located outside this photograph, at a distance of 149 cm. The ends of the tube were closed on the left with a flange made of dielectric, and on the right — made of stainless steel. The electrode 4 was electrically connected to a flat metal plate of the experimental stand. It should be noted that the position of the quartz tube relative to the experimental stand had no effect on the formation of PDJ. When it was installed vertically relative to the Earth surface and the flat plate of the stand, the PDJs were also formed and propagated in both directions from the operating ring electrodes (Fig. 9, in [19]).

This arrangement of electrodes and a long quartz tube were chosen specifically for measuring the emission spectrum of PDJ, which was not affected by an increase in the discharge current through the grounded right flange at the end of the quartz tube. Under the conditions corresponding to Fig. 6, only left PDJ reached the flange 1, and the right PDJ ended at a distance of  $\sim 80$  cm from the electrode 4, without reaching the right metal end. High voltage pulses of positive or negative polarity were applied to the electrode 3. The radiation spectra obtained for these conditions using two spectrometers from PDJ region located on the right at a distance of 21 cm from the electrode 4 are shown in Fig. 7. For spectra shown in Fig. 7 the high-voltage electrode 3 had positive polarity and electrode 4 was grounded. The change in the polarity of electrode 3 had no significant effect on PDJ emission spectrum. It follows from the



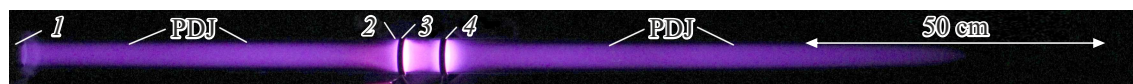


**Figure 6.** Photo of integral luminescence of plasma of the two plasma diffusion jets (PDJ) formed simultaneously in the 220 cm long tube under air pressure of  $p = 1$  Torr. 1 — left flange made of dielectric, 2 — low luminescence in the quartz tube wall, 3 and 4 — outer ring electrodes made of foil. Voltage amplitude between electrodes 7 kV,  $f = 1$  kHz.

spectrogram in Fig. 7, *a* that the highest spectral energy density in the wavelength range  $\Delta\lambda = 250\text{--}1000$  nm lies in the bands of the second positive ( $2+$ ) system  $C^3\Pi_u - B^3\Pi_g$  of molecular nitrogen  $N_2$ . At that, similar to papers [19–22], maximal  $W$  is detected in the band with  $\lambda = 337.1$  nm (vibration transition  $0-0$ ). For the strongest bands of  $1+$  nitrogen system (transition system  $B^3\Pi_g - A^3\Sigma_u^+$ ),  $W$  which is by an order of magnitude lower was detected. However, as can be seen from Fig. 6, as well as from the figures given in papers [19–22], the radiation of  $1+$  bands of the nitrogen system gives a red hue to PDJ glow at low air pressure ( $< 2$  Torr). For the left PDJ the emission spectra at a distance of 21 cm from the electrode 3 had the same distribution of energy spectral density. By changing conditions of excitation, pressure, and decreasing relative humidity, it is possible to improve the PDJ color consistency with the color of the column sprites formed in the upper layers of the Earth's atmosphere.

The emission spectra when shooting from the discharge region located at a distance of 1 cm from the left edge of the high-voltage electrode 3 of negative polarity are shown in Fig. 8. The polarity of the voltage pulses did not significantly affect the emission spectra from the plasma regions at short distances from the electrodes. In the near-electrode area, as was expected, the emission intensity of the first negative band ( $1-$ ;  $B^2\Sigma_u^+ - X^2\Sigma_g^+$ ) of molecular nitrogen ion system  $N_2^+$  (line with the wavelengths of 391.4, 427.8 and 470.9 nm) increased significantly. At that, the ratios of  $R_{391/337}$  and  $R_{391/394}$  of the peak intensities of emission of molecular nitrogen ion  $N_2^+$  ( $\lambda = 391.4$  nm) and nitrogen molecule  $N_2$  ( $\lambda = 337.1$  nm and  $\lambda = 394.3$  nm) are also rising. This indicates a high intensity of the reduced electrical field in this region and, accordingly, a higher electron temperature [19–21]. In this region, as well as in PDJ, the difference between the most intense emission bands of  $2+$  and  $1+$  of the nitrogen systems is very large, only three times less than in Fig. 7, *a*. However, the ratio of the intensity bands ( $1-$ ) of the emission of a molecular nitrogen ion and a nitrogen molecule ( $2+$ ) in the near-electrode region has changed significantly. It followed from the experiments that  $W$  of bands  $1-$  of the nitrogen system at both edges of the two ring electrodes were high and could exceed  $W$  of bands  $2+$  of the nitrogen system at short distances from the electrode edge, where the largest reduced electric field occurs. Note that the near-electrode discharge region does not belong to PDJ, it is a continuation of the barrier discharge plasma region in the tube between the outer ring electrodes, which initiates and forms PDJ.

Due to the high reduced electrical field in the discharge region near the electrodes sharp edge, the lines of atomic oxygen (777.1, 844.6 nm) and hydrogen (656.3 nm) appear in the emission spectra with decreasing air pressure, as well as CO, CO<sub>2</sub> and other bands (see paper [20], which shows the emission spectra at high electrical fields). These lines and bands may also be observed in red sprites [11].

## Discussion of the results

For clarity, when discussing the results obtained in this paper, we use the photo of column sprites shown in Fig. 9. Column red sprites are generally detected not as one „column“, but as several parallel „channels“, spreading downward. In this case, the shape of a separate channel can be very simple, as shown in Fig. 9. This form is close to the form of PDJ, which we observe in experiments. It is well known that the shapes of red sprites differ in variety and size. In literature the following designations of different sprites may be found: column [9–11], carrot [26], angel [27]. For comparison with our experimental data, we chose the simplest column sprites in shape. As a rule, they originate from the bottom of the halo and spread downward due to the positive streamer [11,20]. The downward movement of the streamer initiates a sharp increase in the electrical field between the halo (prevailing positive charge) and the upper layer of thunderstorm clouds (a sharp increase in the negative charge). This usually occurs when lightning develops from a positively charged cloud towards the Earth after a bounced shock [1,2,20]. The positive streamer forms a column sprite that is propagating downward. In later stages, a negative streamer may be initiated from the upper part of the „column“ which is propagating upward from the Earth's surface [27]. Figure 9 shows sprites the development of which ends before the formation of negative streamers. However, for some of them, beads are visible after the dark area at the bottom of the sprite 3. Moreover, some „columns“ have more bright stretching areas (glow areas) 4.

The performed studies made it possible to obtain, when discharged in low-pressure air for analogues of red column sprites, the relationship between the spectral energy density of four different bands. It has been confirmed that the ratio of intensities of individual bands during a repetitively-pulsed discharge that initiates PDJ in a quartz tube depends on the location of their emission and air pressure. It is shown that the spectra and color of the discharge are mostly impacted by the electric field strength, which reaches the highest values at the ring electrodes [20]. Based on this, it can

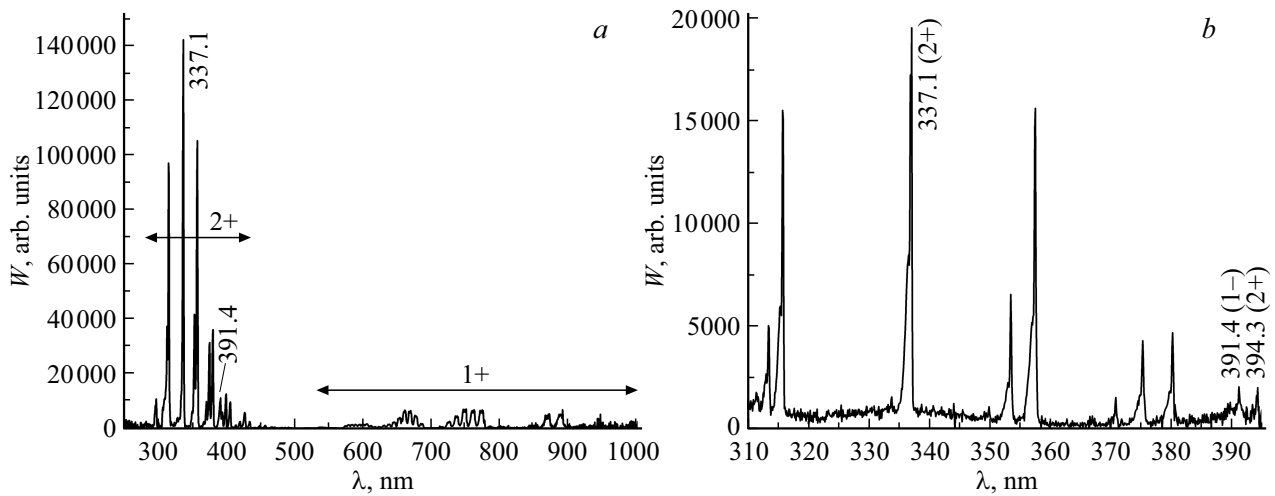


**Figure 7.** Spectral density of PDJ emission energy in the range of  $\Delta\lambda = 250\text{--}1000\text{ nm}$  detected by HR2000+ES spectrometer (a) and in the range of 310–395 nm when detected by HR4000 spectrometer (b) at a distance of 21 cm from the right edge of the grounded electrode 4. Air pressure  $p = 0.3\text{ Torr}$ ,  $f = 2\text{ kHz}$ .

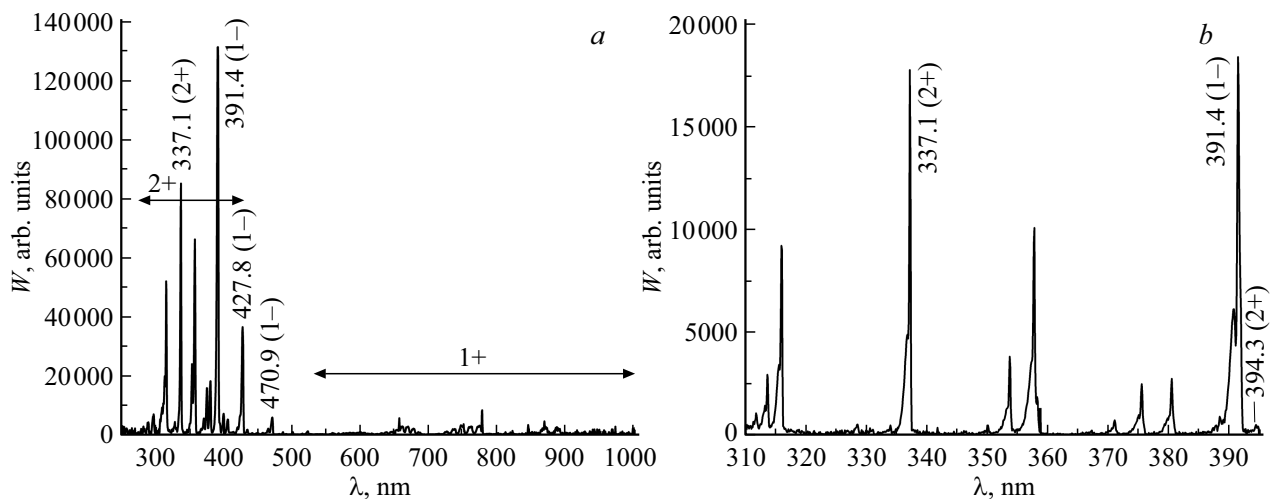


**Figure 8.** Spectral density of PDJ emission energy in the range of  $\Delta\lambda = 250\text{--}1000\text{ nm}$  detected by HR2000+ES spectrometer (a) and in the range of 310–395 nm when detected by HR4000 spectrometer (b) at a distance of 1 cm from the left edge of the high-voltage negative electrode 3. Air pressure  $p = 0.3\text{ Torr}$ ,  $f = 2\text{ kHz}$ .

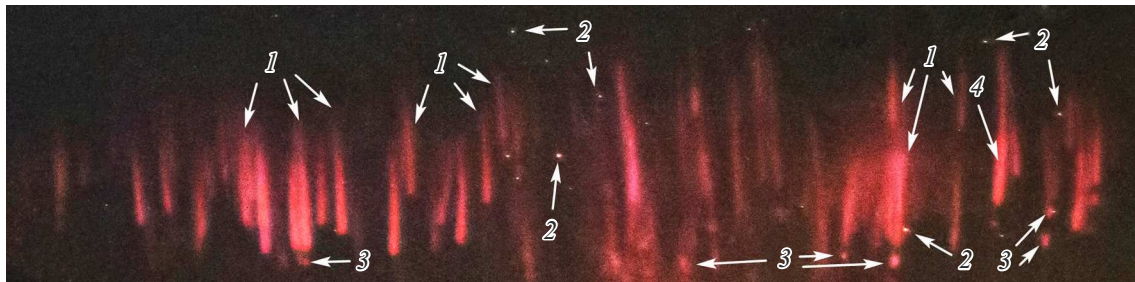


**Figure 9.** A photo of column red sprites, which was obtained by a TLE researcher, a professional photographer, Frankie Lucena. The photo was made on 1 October 2016 above the thunderstorm area in Cabo Rojo, Puerto Rico. 1 — column sprites, 2 — the most bright stars used for calibration of atmospheric radiance of red sprites, 3 — beads, 4 — individual glow areas.



be clearly stated that in paper [12], an increase in the ratio of intensity of the band with a wavelength of 427.8 nm (1-) to the intensity of the band with a wavelength of 337.1 nm with the altitude going down from 60 to 50 km is caused by a higher electrical field strength. Sprites of blue color were observed at altitudes below 50 km as described in papers [28].

The ratios of spectral energy densities in various wavelength ranges, including VUV region, are also very important for determining the main processes occurring in red sprites. The results show that these ratios vary in different areas of the discharge primarily due to differences in the reduced electrical field. Apparently, the main sprites columns are incorporating the secondary streamers formed in the near-sprite atmospheric regions. Because of their formation the color and shape of sprite „columns“ is changed. In particular, the streamers may appear due to the separation of charges in silver clouds, which consist of ice crystals [29]. In PDJ at a distance from the electrodes, the emission spectra and the color of PDJ do not change significantly, which is due to preservation of their propagation conditions. The change in spectra and colors occurs in the areas near the electrodes and at the end of PDJ.

Detailed measurements of the emission spectra during formation of individual PDJ, as well as experimental modeling of various conditions for simulation of glow regions during collision of streamers [30] will help to clarify the physical mechanisms of sprites formation. In particular, such studies will be useful to explain the appearance of glow and bead regions in red sprites, as well as the differences in their shapes.

## Conclusions

The emission of the four most intense nitrogen band systems (2+, 1+, 1-, and LBH) was studied using a setup designed to produce PDJ in air and nitrogen. The emission was also detected on atomic lines of nitrogen, oxygen and hydrogen. These bands and lines, as well as bands of other molecules and ions, are present during low-pressure discharges in the air and, with increasing sensitivity of the measurement system, are likely to be detected in the spectra of red sprites, as well as other TLE [1,2,11].

For 2+ and 1- bands of the nitrogen systems, as well as for VUV transitions the LBH emission was detected for both of them at a time. The data obtained also make it possible to clarify the results of detailed computation for different nitrogen bands, which are given in [14] for a wide range of reduced electrical field strengths. At the same time, both the consistency of calculated and experimental trends, as well as their difference should also be emphasized.

It has been established that emission of LPH bands is detected in PDJ at various air pressures, despite the strong absorption of molecular oxygen. This result is consistent with the conclusion of [31] that emission of this band plays

an important role in advancing the ionization wave into unexcited gas due to photoionization. The presence of VUV emission also explains the higher uniformity of pulsed discharges in nitrogen compared to discharges in air, which is observed with nanosecond high-pressure discharges [32]. We assume that the results obtained can be useful in studying the spectral characteristics of red sprites and other TLE.

## Acknowledgments

The authors of the article express their gratitude to professional photographer Frankie Lucena for providing the photos and permission to use it in this article, and also thank D.S. Pechenitsyn for development of a repetitively-pulsed generator and D.A. Sorokin for supporting this study.

## Funding

This study was carried out under the state assignment of the Institute of High Current Electronics of the Siberian Branch of the Russian Academy of Sciences on the subject № FWRM-2021-0014.

## Conflict of interest

The authors declare that they have no conflict of interest.

## References

- [1] V.V. Surkov, M. Hayakawa. *Surv. Geophys.*, **41** (5), 1101 (2020). DOI: 10.1007/s10712-020-09597-2
- [2] F.J. Gordillo-Vázquez, F.J. Pérez-Invernón. *Atm. Res.*, **252**, 105432 (2021). DOI: 10.1016/j.atmosres.2020.105432
- [3] H.C. Stenbaek-Nielsen, M.G. McHarg, R. Haaland, A. Luque. *J. Geophys. Res. Atmos.*, **125**, e2020JD033170 (2020). DOI: 10.1029/2020JD033170
- [4] C.L. Kuo, E. Williams, T. Adachi, K. Ihaddadene, S. Celestin, Y. Takahashi, R.R. Hsu, H.U. Frey, S.B. Mende, L.C. Lee. *Front. Earth Sci.*, **9**, 687989 (2021). DOI: 10.3389/feart.2021.687989
- [5] R.C. Franz, R.J. Nemzek, J.R. Winckler. *Science*, **249**, 48 (1990).
- [6] D.D. Sentman, E.M. Wescott, D.L. Osborne, D.L. Hampton, M.J. Heavner. *Geophys. Res. Lett.*, **22**, 1205 (1995).
- [7] G.K. Garipov, B.A. Khrenov, P.A. Klimov, V.V. Klimenko, E.A. Mareev, O. Martines, E. Mendoza, V.S. Morozenko et al. *J. Geophys. Res.: Atmosph.*, **118**, 370 (2013).
- [8] A. Jehl, T. Farges, E. Blanc. *J. Geophys. Res.: Space Phys.*, **118**, 454 (2013).
- [9] C. Köhn, O. Chanrion, T. Neubert. *J. Geophys. Res.: Space Phys.*, **124**, 3083 (2019).
- [10] M.B. Garnung, S. Celestin, T. Farges. *J. Geophys. Res.: Space Phys.*, **126**, e2020JA028824 (2021).
- [11] V.P. Pasko. *Plasma Sources Sci. Technol.*, **16** (1), S13 (2007). DOI: 10.1088/0963-0252/16/1/S02
- [12] J. Morrill, E. Bucsele, C. Siefing, M. Heavner S.D. Moudry, S. Slinker, D. Fernsler, E. Wescott, D. Sentman, D. Osborne. *Geophys. Res. Lett.*, **29** (10), 1462 (2002). DOI: 10.1029/2001GL014018

- [13] H.C. Stenbaek-Nielsen, M.G. McHarg, T. Kanmae, D.D. Sentman. *Geophys. Res. Lett.*, **34**, L11105 (2007). DOI: 10.1029/2007GL029881
- [14] F. Jiang, C. Huang, Y. Wang. *Meteorol. Atmosph. Phys.*, **131**, 421 (2019).
- [15] A.S. Kirillov, V.B. Belakhovsky. *Geomagn. Aeron.*, **60**, 781 (2020). DOI: 10.1134/S0016793220060079.
- [16] Y. Goto, Y. Ohba, K. Narita. *J. Atmosph. Electr.*, **27** (2), 105 (2007). DOI: 10.1541/jae.27.105
- [17] A. Robledo-Martinez, A. Garcia-Villarreal, H. Sobral. *J. Geophys. Res.: Space Phys.*, **122**, 948 (2017). DOI: 10.1002/2016JA023519
- [18] F.C. Parra-Rojas, M. Passas, E. Carrasco, A. Luque, I. Tanarro, M. Simek, F.J. Gordillo-Vázquez. *J. Geophys. Res.: Space Phys.*, **118** (7), 4649 (2013). DOI: 10.1002/jgra.50433.
- [19] V. Tarasenko, N. Vinogradov, E. Baksht, D. Sorokin. *J. Atmosph. Sci. Res.*, **5** (03), 26 (2022). DOI: 10.30564/jasrv5i3.4858
- [20] V.F. Tarasenko, E.Kh. Baksht, N.P. Vinogradov, D.A. Sorokin. *Opt. Spectrosc.*, **130** (12), 1499 (2022). DOI: 10.21883/EOS.2022.12.55234.4014-22.
- [21] D.A. Sorokin, V.F. Tarasenko, E.Kh. Baksht, N.P. Vinogradov. *Physics of Plasmas*, **30** (8), 083515 (2023). DOI: 10.1063/5.0153509
- [22] V.F. Tarasenko, E.K. Baksht, V.A. Panarin, N.P. Vinogradov. *Plasma Physics Reports*, **49** (6), 786 (2023). DOI: 10.1134/S1063780X23700393.
- [23] V.S. Skakun, V.F. Tarasenko, V.A. Panarin, D.A. Sorokin. *Instruments and Experimental Techniques*, **67** (3), 519 (2024). DOI: 10.1134/S0020441224700817.
- [24] G.N. Gerasimov. *Physics-Uspekhi*, **47** (2), 149 (2004). DOI: 10.1070/PU2004v047n02ABEH001681.
- [25] B. Zhang, Y. Zhu, X. Zhang, N. Popov, T. Orri re, D.Z. Pai, S.M. Starikovskaia. *Plasma Sources Sci. Technol.*, **32** (11), 115014 (2023). DOI: 10.1088/1361-6595/ad085c
- [26] A. Malagon-Romero, J. Teunissen, H.C. Stenbaek-Nielsen, M.G. McHarg, U. Ebert, A. Luque. *Geophys. Res. Lett.*, **47**, e2019GL085776 (2020). DOI: 10.1029/2019GL085776
- [27] W. Lyons. *Weatherwise*, **75** (6), 14 (2022). DOI: 10.1080/00431672.2022.2116249
- [28] T. Kanmae, H.C. Stenbaek-Nielsen, M.G. McHarg, R.K. Haaland. *Geophys. Res. Lett.*, **37**, L13808 (2010). DOI: 10.1029/2010GL043739
- [29] M. Hervig, R.E. Thompson, M. McHugh, L.L. Gordley, J.M. Russell III, M.E. Summers. *Geophys. Res. Lett.*, **28**, 971 (2001). DOI: 10.1029/2000GL012104
- [30] V.F. Tarasenko, N.P. Vinogradov, E.Kh. Baksht, D.A. Sorokin, D.S. Pechenitsin. *Atmospheric and Oceanic Optics*, **37** (4), 547 (2024). DOI: 10.1134/S1024856024700738.
- [31] A. Fierro, J. Lehr, B. Yee, E. Barnat, C. Moore, M. Hopkins, P. Clem. *J. Appl. Phys.*, **129** (7), 073302 (2021). DOI: 10.1063/5.0033412
- [32] V.F. Tarasenko (ed.). *Runaway Electrons Preionized Diffuse Discharges* (Nova Science Publishers, Inc., NY, 2014).

*Translated by T.Zorina*